Desalination and Water Treatment
www.deswater.com
doi: 10.5004/dwt.2023.30199

316 (2023) 327–334
December

Polycationic liquid modified functional membrane showing good separation performance in dye wastewater treatment

Minyan Wu[a], Zirui Wang[b], Shumeng Liu[a], Qing Zhang[b], Xiaoji Zhou[b,c], Shusu Shen[b,c,*]

[a]*Suzhou Environmental Monitoring Station, Suzhou, China, Tel.: +86 51268092987; emails: 88611620@qq.com (M. Wu), 928760553@qq.com (S. Liu)*
[b]*School of Environmental Science and Engineering, Suzhou University of Science and Technology, Suzhou, China, Tel.: +86 51268092987; emails: shusushen@mail.usts.edu.cn (S. Shen), 648657802@qq.com (Z. Wang), 1474835245@qq.com (Q. Zhang), 359300091@qq.com (X. Zhou)*
[c]*Jiangsu Engineering Research Center for Separation and Purification Materials and Technology, Suzhou, China*

Received 8 September 2023; Accepted 29 November 2023

ABSTRACT

Membrane separation technology is widely used in the treatment of dye wastewater because of its low cost, high separation efficiency, simple operation and no secondary pollution. In this study, a series of blend cellulose acetate (CA) membranes with different compositions were prepared by blending a polycationic liquid synthesized in laboratory with CA. The membranes were characterized by Fourier-transform infrared spectroscopy, scanning electron microscopy analysis and the surface properties including the water contact angle, mechanical strength, pure water flux, pore size and zeta potentials were also tested. The hydrophilicity of the membrane was improved by blending more additive. Compared with pure CA membrane, the surface zeta potential value of the modified membrane increased. The maximum pure water flux of the modified membranes was 32.51 L/m^2·h. In the experiment of filtering two cationic dyes (acridine yellow hydrochloride and Rhodamine B) with different molecular weights, it is found that the blend modified membrane with optimal performance showed better antifouling performance and higher rejection rate, the flux recovery rates of acridine hydrochloride yellow and Rhodamine B were 93.94% and 87.47%, and the rejection rates were 87% and 76.1%, respectively.

Keywords: Cellulose acetate; Membrane separation; Blending modification; Water treatment; Dye removal

1. Introduction

Membrane separation technology has great potential in water and wastewater treatment. Based on the pore size diameter, membranes are often classified into microfiltration membranes, ultrafiltration membranes, nanofiltration membranes, and reverse osmosis membranes [1–4]. According to different membrane materials, membranes can be divided into inorganic membranes, organic membranes, or organic–inorganic hybrid membranes. Among various matrix membrane materials, cellulose acetate (CA) is the earliest membrane material due to its easy modification, low cost, good membrane-forming ability, and excellent hydrophilicity [5–10].

However, due to the dense surface layer and low porosity, CA membranes produce very little flux [11]. In addition, CA membranes also have some disadvantages, such as low mechanical strength, narrow temperature (up to 30°C) and pH operating range, and highly susceptible to biological and organic pollutants [12]. To achieve antifouling CA membranes, different kinds of modifications have been developed. The modification methods mainly include

* Corresponding author.

membrane surface modifications such as surface coating [13,14] or surface grafting [15,16], and membrane bulk modifications such as copolymerization modification [17–19] or blending modification [20,21]. Among them, blending modification not only has the physical and chemical properties of the original membrane, but also has the function of the added blend [22], so that a more ideal membrane material can be obtained.

Polyionic liquids, also known as polymer ionic liquids [23], not only retains the ionic liquid's strong conductivity, high thermal stability and non-flammability, but also combines the polymer's processability, easy recycling, high mechanical stability and other excellent properties, so they are quite applicable in solving the membrane modification problem [24–27].

In previous reports, membranes prepared by blending polycationic liquids P(PEGMA$_m$-co-BVIm-Br$_n$) (m/n = 2/1 or 1/1) with polyvinylidene fluoride (PVDF) showed excellent removal of contaminants including proteins, dyes and oils [28–30]. However, the prepared membranes had relatively large pore sizes and PVDF was a hydrophobic material, which could easily cause membrane contamination. Therefore, in this study, CA, which is highly hydrophilic and relatively dense, was selected as the substrate, and polycationic liquids were used as additives to prepare polycationic liquid modified functional membranes by non-solvent-induced phase separation (NIPS) method. The surface properties were carefully investigated by adjusting the preparation parameters, including the casting solution composition and the blending ratio. In addition, the preliminary application of the membranes in the treatment of dye containing wastewater was also studied.

2. Experimental set-up

2.1. Chemicals

Cellulose acetate (CA) and N,N-dimethylformamide (DMF, AR) were obtained from Aladdin Chemical Co., Ltd., (Shanghai, China). Poly(ethylene glycol) methyl ether methacrylate (PEGMA, average Mn 950, contains 300 ppm butylated hydroxytoluene and 100 ppm 4-methoxyphenol as inhibitor) was purchased from Aldrich (Shanghai, China). Vinylimidazole ($C_5H_6N_2$, 99%) and 1-bromobutane (C_4H_9Br, >99%) were purchased from Shanghai Adamas Reagent Co., Ltd., (Shanghai, China). Dimethyl sulfoxide (DMSO) was supplied by Tianjin Zhiyuan Chemical Reagent Co., Ltd., (China). Other chemicals utilized in this study were all purchased with analytical quality and purified before use. Deionized (DI) water (18.2 MΩ) purified with a Milli-Q system from Millipore (Burlington, MA, USA) was used to prepare all solutions as needed in the work.

2.2. Preparation of membranes

The polycationic liquid, names as P in this report, was synthesized according to the previous procedure [31] by reaction between 1-butyl-3-vinylimidazole bromide (BVIm-Br) and PEGMA *via* Reversible Addition-Fragmentation Chain Transfer Polymerization (RAFT) reaction, and the structure is shown in Fig. 1. It has been characterized by Fourier-transform infrared spectroscopy (FTIR) and ^{1}H NMR, and the characterization results are completely consistent with the literature reports. In this work, six flat sheet membranes were prepared by blending polycationic liquid with CA in different weight ratios, *via* a NIPS method. Firstly, the polycationic liquid and CA were incorporated into DMSO and stirred (350 rpm) for 24 h at 60°C in an oil bath to afford homogeneous casting solution. The casting solution was cooled to room temperature and centrifuged to remove air bubbles at 8,000 rpm. Afterwards, the defoamed solution was cast on a glass plate through a film scraper with 300 μm thickness. After exposed to air for 10 s, the film was transferred into a coagulation bath for 2 h. After accomplished inversion process, the formed membrane was stored in water for 24 h and take it out to dry naturally to use later. The compositions of the casting solution are summarized in Table 1.

2.3. Characterization of membranes

2.3.1. FTIR spectroscopy

FTIR model (Nicolet iS10) was used to analyze the surface functional groups of the membranes, with a spectral range of 500~4,000 cm^{-1} and a resolution of 4 cm^{-1}.

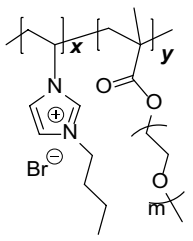

P(BVImBr-*co*-PEGMA)

Fig. 1. Chemical structure of polycationic liquid, P [31].

Table 1
Composition of the membrane casting solution

Membranes	Weight ratio of CA/P	Polymer concentration/wt.%	Solvent concentration/wt.%	Coagulation bath
M0	20:0	18	DMSO/82	DI water
M1	20:1	18	DMSO/82	
M2	20:2	18	DMSO/82	
M3	20:0	20	DMSO/80	
M4	20:1	20	DMSO/80	
M5	20:2	20	DMSO/80	

2.3.2. Morphological analysis

Surface and cross-sectional morphologies of membrane samples were observed with scanning electron microscopy (SEM; Carl Zeiss EVO 18, Germany). The membrane that was brittle in liquid nitrogen was fixed on the sample stage with conductive adhesive, and after spraying gold, it was placed in a scanning electron microscope and evacuated for observation.

2.3.3. Thermogravimetric analysis and zeta potential

An Rigaku analyzer was used for thermogravimetric analysis (TGA). The membrane surface charge properties were measured with a membrane solid sample flow field potential analyzer (Surpass 3).

2.3.4. Pure water flux

The pure water flux test was carried out by using a homemade dead-end filtration device from the laboratory. The membrane to be tested was cut into original pieces of a certain size and was fixed in an ultrafiltration cup with an effective filtration area of 8.55 cm^2. At first, the membrane was pretreated under 0.8 MPa for 30 min, and second, the pure water was filtered under 0.7 MPa and the filtered pure water was collected at intervals. The pure water flux J_w was calculated by Eq. (1) [32] until the effluent volume was stable.

$$J_w = \frac{V}{St} \tag{1}$$

where J_w is the pure water flux ($L/m^2 \cdot h$), V is the volume of pure water across the membrane (L), t is the time of each water withdrawal (h), and S is the effective membrane area of water across the membrane (m^2).

2.3.5. Porosity and pore size

The membrane porosity was measured by the weighing method: the membrane to be tested was cut into circular slices with a diameter of 1.0 cm, which was washed in absolute ethanol and then soaked in deionized water (DI water) for 24 h. Take out the soaked membrane and wipe the residual moisture on the membrane surface with a dust-free paper. Weigh the wet membrane mass with an electronic balance (Gubis, Sartorius, Germany) and record as W_2. The wet membrane was placed in a vacuum drying oven at 60°C and dried until the membrane quality was stable and then taken out. The dry membrane mass at this time was weighed and recorded as W_1. The membrane porosity ε was calculated by Eq. (2) [33]:

$$\varepsilon = \frac{w_2 - w_1}{\rho A d} \times 100\% \tag{2}$$

where ε represents the porosity (%), W_1 and W_2 are the wet weight and dry weight (kg), ρ represents the density of water (kg/m^2), A is the area (m^2) and d is the thickness (m) of the membrane.

The average pore size (r_m) of the membrane is calculated with the aid of the Guerout–Elford–Ferry formula based on pure water flux and porosity data. The average pore size (r_m) of the membrane was determined by Eq. (3) [33,34]:

$$r_m = \sqrt{\frac{(2.9 - 1.75\varepsilon) \times 8\eta l Q}{\varepsilon A \Delta p}} \tag{3}$$

where r_m (μm) is the average pore size, ε (%) is the porosity, η (8.9×10^{-4} Pa·s) is the liquid viscosity, l (cm) is the thickness of the membrane, Q (cm^3/s) is the volume of pure water permeating through the membrane per unit of time, A (cm^2) is the surface area of the membrane, and Δp (10^5 Pa) is the operating pressure.

2.3.6. Mechanical characterization and water contact angles

The mechanical strength was tested by a tensile strength tester (5944, Instron, Norwood, MA, USA); 3 to 5 strips of 5 cm × 1 cm were measured from different positions, and the average value was recorded.

The static water contact angle was measured by the static hanging drop method, with a membrane surface contact angle tester (Ramé-Hart 500). The contact angle was measured at 5 different positions on each sample, the average value was calculated and recorded with the obtained data, and the accepted error range was less than 3.

2.3.7. Filtration experiments

Acridine yellow hydrochloride (AH, Mw = 505.4) and Rhodamine B (RhB, Mw = 479.01) were selected for the anti-dye contamination experiment. The flux recovery rate (FRR) was calculated by Eq. (4) [34], and the rejection (R) was calculated by Eq. (5) [32–34]:

$$\mathrm{FRR} = \frac{J_r}{J_w} \times 100\% \tag{4}$$

$$R = 1 - \frac{C_e}{C_0} \times 100\% \tag{5}$$

where J_w is the pure water flux of the membrane, J_r is the recovery flux of the membrane, C_o is the contaminant concentration in the feed solution (mg/g), and C_e is the contaminant concentration in the filtrate (mg/g).

3. Results and discussion

3.1. Surface chemical composition of the membranes

FTIR analysis was conducted to determine the surface chemical composition of the membranes and the spectra is shown in Fig. 2. Compared with the pristine CA membranes M0 and M3, the blend membranes M1, M2, M4, and M5 showed characteristic peaks near 1,738.8 and 2,866.6 cm^{-1}, which can be assigned to the C=O absorption peaks and the C–H stretching vibration in polycationic liquid P, respectively; 1,432.4 cm^{-1} was the characteristic absorption peak of C–N vibration in the imidazolium ring skeleton;

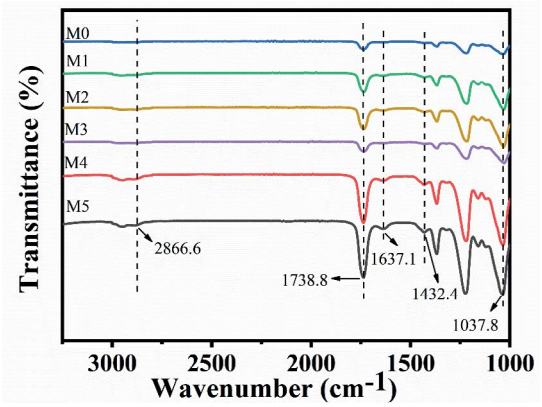

Fig. 2. Fourier-transform infrared spectra of the membranes.

1,037.8 cm^{-1} can be assigned to the C–O characteristic peaks in PEGMA. Also, the intensity of these peaks increased with more adding of the polycationic liquid, indicating that the polycationic liquid was successfully blended with CA.

3.2. Morphology of the membranes

Fig. 3 shows SEM images of the membrane surface and cross-sectional morphology, on the left is the surface of the membrane magnified 50,000 times, and on the right is a cross-sectional view magnified 250 times. No obvious pore can be found on the surface of pure CA membrane (M0). Comparably, more pores appeared on the surface of the blended membranes. This is mainly due to the hydrophilic polycationic liquid (P) that may accelerate the mass transfer rate of the solvent and non-solvent during the phase transfer stage, partial amount of P might leach out from the flat sheet, thus producing a more porous and loose membrane structure. It can be seen from the cross-sectional view that the blend membranes (M1, M2, M4, M5) all became thicker with an increased ratio of the polycationic liquid (P). The thicknesses of membranes M0, M1, M2, M4 and M5 were 103, 111, 192, 203, 215 and 192 μm, respectively, which is mainly due to the increased concentration of the casting solution, delaying the exchange between the solvent and the non-solvent, and ultimately forming a sponge-like structure.

3.3. Thermal stability and zeta potentials of the membranes

TGA curves of M3-M5 are described in Fig. 4a. From the figure it can be seen that the pure CA membrane M3 showed the only thermal weight loss at 280°C, which may be due to water decomposition. The modified membranes M4 and M5 both showed three thermal weight loss processes. The first stage of the weight loss process (before 300°C) was attributed to the decomposition of water adsorbed by the membranes, the second stage of the weight loss (300°C ~ 400°C) was mainly due to the decomposition of polycationic liquids in the membranes, and the third stage of the decomposition (after 400°C) was attributed to the decomposition of the CA skeleton. It also can be found that the thermal stability of the modified membrane decreased with the increase of polycationic liquid addition in the modified membrane.

The zeta potential data of the M3 and M4 membrane are shown in Fig. 4b for pH in the range of 3–10. Due to the addition of the cationic additive P, the membrane surface zeta potential value increased, but the CA membrane surface was still negatively charged, which may be due to the small amount of polycationic liquid added. This increased positive charge on the membrane surface may help to enhance the electrostatic interaction between the membrane surface and pollutants in wastewater, which is quite beneficial for the interception effects of the membrane on some charged pollutants.

3.4. Porosity, pore size and pure water flux

As shown in Table 2, the pure water flux of the modified membranes increased with increasing polycationic liquid content at the same casting liquid concentration compared to the pure CA membranes M0, this is due to the porosity of the membranes and the hydrophilic of the additives, which allowed water to pass through the membrane with lower resistance. No water flux was detected for membrane M0 because it is a compact membrane, and this can be found from the SEM images in Fig. 3. By mixing with the polycationic liquid, more pores appeared and the porosity was enlarged greatly from 1.75% (M0) to 92.56% (M2). Both the porosity and the average pore size of the membranes increased with the increase of the polycationic liquid content, this is mainly due to the increased content of hydrophilic polycationic liquids, which accelerated the exchange rate between solvent and non-solvent. Compared with other blend membranes, M4 gave smaller pore size (0.00664 nm) and lower pure water flux (6.9 $L/m^2 \cdot h$), and it can be found that membrane M4 had a denser structure and fewer pores on the membrane surface. These data are accorded with SEM observations as shown in Fig. 3.

3.5. Mechanical property

The mechanical properties of the membranes are shown in Fig. 5. The mechanical strength of the membranes M2 and M5 decreased with increasing amount of polycationic liquid at the same concentration of the casting liquid. This is mainly due to the fact that with the increase of the addition of polycationic liquid, the exchange between solvent and non-solvent was accelerated in the film-forming stage, resulting in the increase of finger-like pores in the surface of membranes, as well as the formation of membrane pores during the migration of hydrophilic polycationic liquid to the solidification bath in the process of phase transition. It shows that the structure of CA membrane could be changed by the addition of polycationic liquid and led to the weakening of mechanical properties. In addition, under the same blending ratio, the mechanical properties of the membranes were enhanced by the reduction of finger-like macropores in the membranes due to the delayed solvent-nonsolvent exchange with the increase of the concentration of the casting polymer.

3.6. Water contact angle

The water contact angles of the membranes are shown in Fig. 6a. The smaller water contact angle represents the

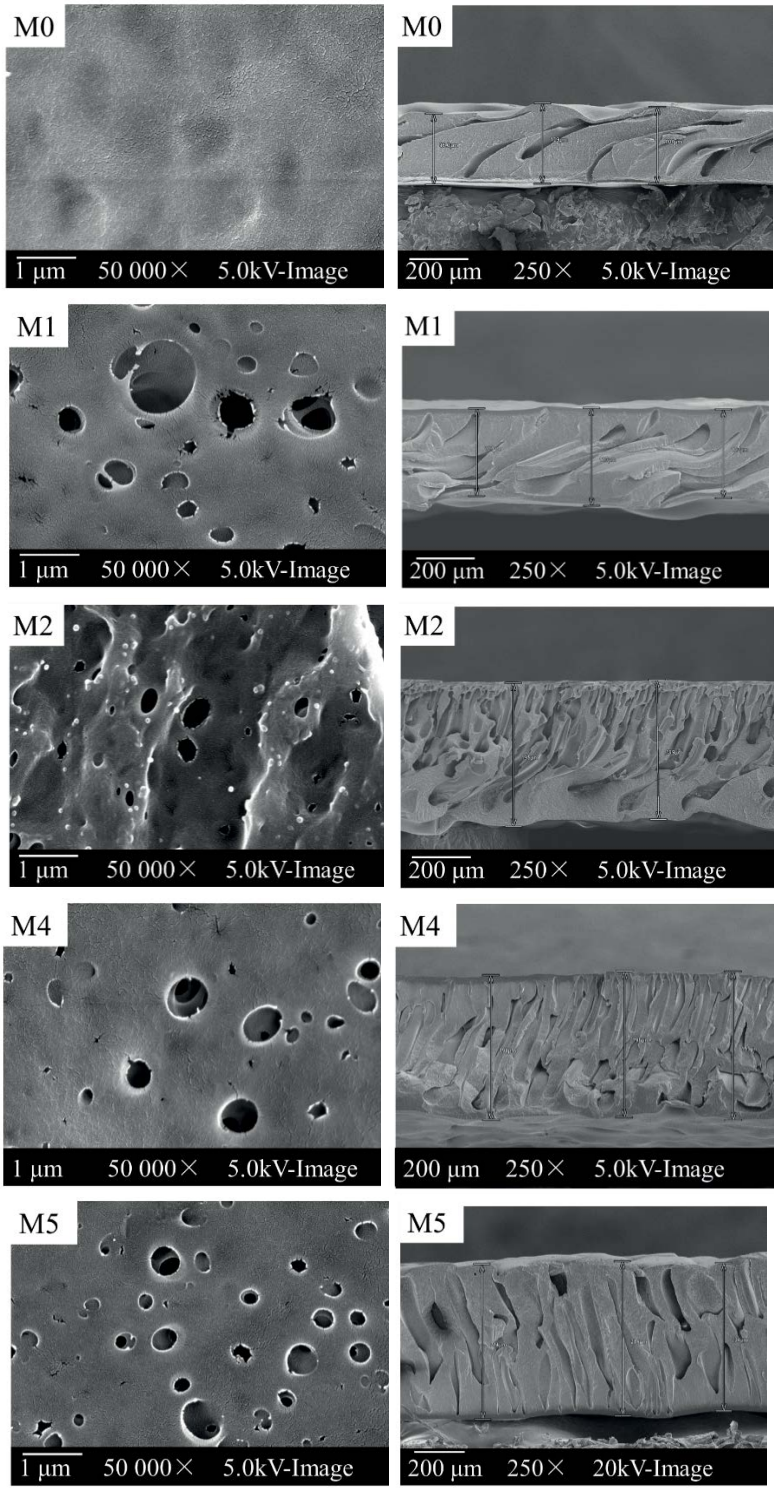

Fig. 3. Scanning electron microscopy images of the upper surface (left) and cross-section (right) of the membranes.

better hydrophilic performance. Compared with the original membranes M0 and M3, the water contact angles of M1 and M2 decreased to 77.9° and 75.4°, respectively. With the addition of polycationic liquid, and the water contact angles of M4, and M5 showed the same pattern, 79.4° and 77.9°, respectively, which indicated that the hydrophilicity of the membranes was increasing. Therefore, the addition of polycationic liquid can enhance the hydrophilicity of membrane surface.

The dynamic water contact angle was further measured for M3, M4 and M5, as shown in Fig. 6b. The faster the wetting rate indicates the better the hydrophilic performance.

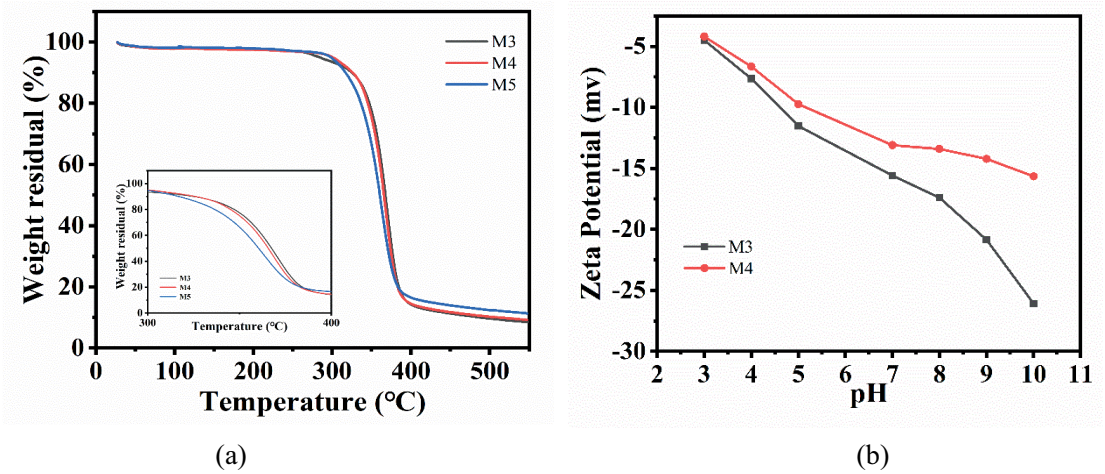

Fig. 4. (a) Thermogravimetric analysis diagram of membranes M3, M4, and M5 and (b) zeta potentials of membranes M3 and M4.

Table 2
Parameters of the original membrane M0 and the blend membrane M1, M2, M4 and M5

Membranes	Porosity (%)	Pure water flux (L/m²·h)	Average pore size (nm)
M0	1.75	/	/
M1	86.52	25.44 ± 1.3	1.863
M2	92.56	32.51 ± 2.2	2.442
M4	85.20	6.90 ± 1.90	0.00664
M5	91.17	10.10 ± 2.60	0.102

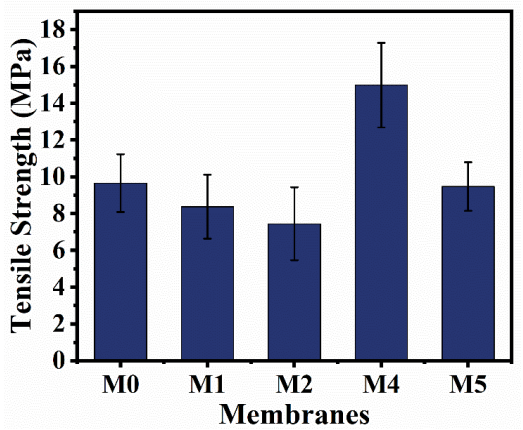

Fig. 5. Mechanical characterization of membranes M0, M1, M2, M4 and M5.

Compared with the original membrane M3, the blend membrane containing polycationic liquid had a faster wetting rate. It was also found that the higher the additive content, the faster the wetting rate of the membranes. Among them, the contact angle of M5 with the most polycationic liquid content was 44.9° at 6 min, which may be attributed to two aspects, one was the addition of hydrophilic additives, and the second was the influence of membrane surface roughness.

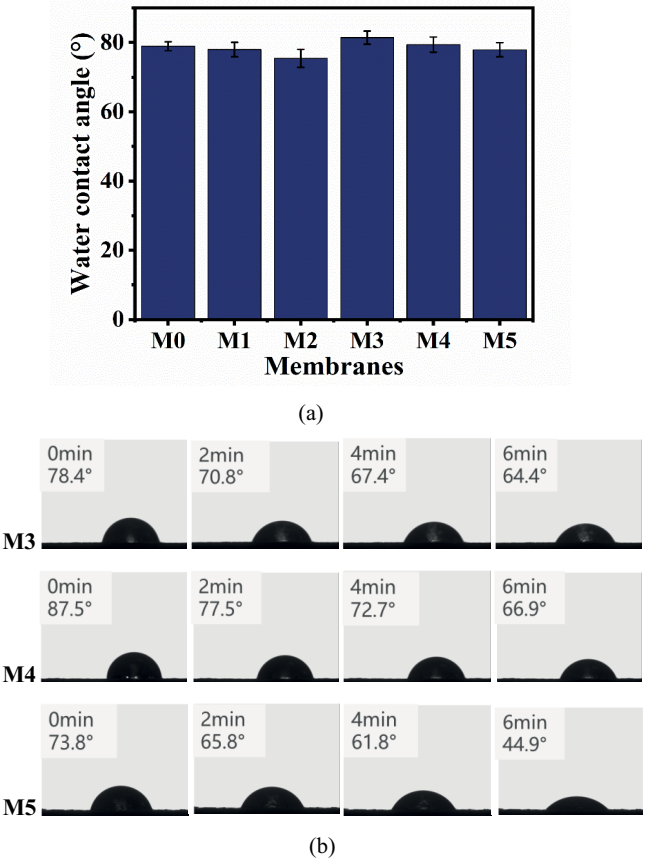

Fig. 6. (a) Static water contact angles of the six membranes and (b) the dynamic water contact angles of membranes M3, M4 and M5.

3.7. Application in the cross-flow filtration of dye water

In the present study, cross-flow filtration experiments were carried out on two different cationic-type dyes, acridine yellow hydrochloride (AH) and Rhodamine B (RhB), at a concentration of 30 mg/g. AH and RhB are quaternary ammonium salts, which existed in the form of quaternary

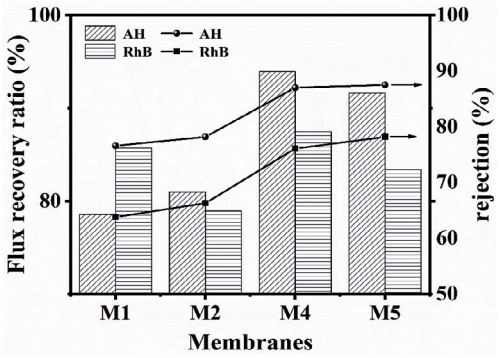

Fig. 7. Rejections and flux recovery ratios of AH and RhB of the blend membranes M1, M2, M4 and M5.

ammonium cation after dissociation, and at the same time, imidazole cation (from polycationic liquid) existed on the surface of the modified membrane, so there was an electrostatic repulsion between the imidazole cation and the quaternary ammonium salts, and the dye molecules in filtration were enriched on the surface of the membrane to form the hydration layer, which caused the membrane pores to be clogged to hinder the passage of dye molecules.

As shown in Fig. 7, the rejection rates of M1, M2, M4 and M5 for AH were 76.60%, 78.20%, 87.00% and 87.50%, respectively; and the rejection *R* of M1, M2, M4 and M5 for RhB were 63.80%, 66.30%, 76.10% and 78.20%, respectively. It shows that the rejection rate of AH was higher than that of RhB, this may be mainly caused by the effect of pore size sieving. The flux recovery rates of AH and RhB for membrane M4 were 93.94% and 87.47%, respectively. In other words, the membrane M4 had better fouling resistance to cationic dyes, which can be explained by the addition of hydrophilic polycationic liquids enhanced the hydrophilicity of the CA membrane, and a hydration layer was formed on the surface of the membrane, which prevented the dye molecules from adhering.

Ong et al. [35] reported a cellulose acetate (CA) microfiltration membrane modified by vacuum filtration-assisted layer-by-layer deposition of bilayers, the dye-rejection performance of the modified membranes increased as increasing bilayers of deposited on the membranes, and the rejection rate of cationic methylene blue (MB) dye was about 80%. Mahmodi et al. [36] prepared a mixed matrix membrane by incorporating hydrophilic MIL-101(Cr)-NH_2 nanoparticles into cellulose acetate (CA) matrix, resulting in enhanced hydrophilicity. The prepared membranes exhibited high rejection (>97%) of methyl blue dye through size exclusion mechanism. In comparison, polycationic liquid modified CA membranes in this work have a good potential for application in dye wastewater treatment under the same substrate condition. However, its application in wastewater treatment is still worthy of further expectation.

4. Conclusion

In this work, a positively charged porous CA membrane was firstly reported and successfully prepared from blending a polycationic liquid and cellulose acetate. Due to the blending of the polycationic liquid additive, the hydrophilicity of the CA membrane was enhanced that the water contact angle was reduced. Compared with pure CA membrane, the membrane porosity and the pure water flux was enlarged to 92.56% and 32.51 L/m^2·h. The membrane surface appeared more positively charged by blending the polycationic liquid. Among all the modified membranes, membrane M4 who has the smallest pore size (0.00664 nm) and water flux (6.9 L/m^2·h) showed good removal effect of two different cationic-type dyes (AH and RhB) in water. On the whole, this study expands the application of polycationic liquid in blended membranes, and realizes the removal of charged pollutants by using its charging property. Using cellulose acetate as the substrate membrane material is environmentally friendly. By using polycationic liquid as an effective modifier for CA, membrane separation materials with denser membrane pore sizes can be prepared, which can be suitable for dyes with very small particle sizes in aquatic environments, and even for heavy metal ions. This provides important data support for the development of efficient membrane technology for treating dyes in water. However, this study is not deep enough, such as the types of pollutants are small, the lack of cyclic experiments, etc. The research team is still exploring the in-depth research.

Acknowledgments

The authors thank the financial support from the National Natural Science Foundation of China (No. 51608342) and Preresearch Fund of Jiangsu Collaborative Innovation Center of Technology and Material of Water Treatment (XTCXSZ2022-9).

References

[1] T. Luo, S. Abdu, M. Wessling, Selectivity of ion exchange membranes: a review, J. Membr. Sci., 555 (2018) 429–454.
[2] W. Wang, J. Sun, Y. Zhang, Y. Zhang, G. Hong, R.M. Moutloali, B.B. Mamba, F. Li, J. Ma, L. Shao, Mussel-inspired tannic acid/polyethyleneimine assembling positively-charged membranes with excellent cation permselectivity, Sci. Total Environ., 817 (2022) 153051, doi: 10.1016/j.scitotenv.2022.153051.
[3] Y. Wang, D. Li, J. Li, J. Li, M. Fan, M. Han, Z. Liu, Z. Li, F. Kong, Metal organic framework UiO-66 incorporated ultrafiltration membranes for simultaneous natural organic matter and heavy metal ions removal, Environ. Res., 208 (2022) 112651, doi: 10.1016/j.envres.2021.112651.
[4] M. Yao, L.D. Tijing, G. Naidu, S.-H. Kim, H. Matsuyama, A.G. Fane, H.K. Shon, A review of membrane wettability for the treatment of saline water deploying membrane distillation, Desalination, 479 (2020) 114312, doi: 10.1016/j.desal.2020.114312.
[5] S. Yang, Q. Zou, T. Wang, L. Zhang, Effects of GO and MOF@GO on the permeation and antifouling properties of cellulose acetate ultrafiltration membrane, J. Membr. Sci., 569 (2019) 48–59.
[6] S.-s. Shen, C. Hao, R.-h. Wang, W. Ji, Y. Zhang, R. Bai, Preparation of antifouling cellulose acetate membranes with good hydrophilic and oleophobic surface properties, Mater. Lett., 252 (2019) 1–4.
[7] M.R. De Guzman, C.K.A. Andra, M.B.M.Y. Ang, G.V.C. Dizon, A.R. Caparanga, S.-H. Huang, K.-R. Lee, Increased performance and antifouling of mixed-matrix membranes of cellulose acetate with hydrophilic nanoparticles of polydopamine-sulfobetaine methacrylate for oil-water separation, J. Membr. Sci., 620 (2021) 118881, doi: 10.1016/j.memsci.2020.118881.
[8] S. Tahazadeh, T. Mohammadi, M.A. Tofighy, S. Khanlari, H. Karimi, H.B.M. Emrooz, Development of cellulose acetate/

metal-organic framework derived porous carbon adsorptive membrane for dye removal applications, J. Membr. Sci., 638 (2021) 119692, doi: 10.1016/j.memsci.2021.119692.
[9] S. Li, X. Wang, Y. Guo, J. Hu, S. Lin, Y. Tu, L. Chen, Y. Ni, L. Huang, Recent advances on cellulose-based nanofiltration membranes and their applications in drinking water purification: a review, J. Cleaner Prod., 333 (2022) 130171, doi: 10.1016/j.jclepro.2021.130171.
[10] V. Vatanpour, M.E. Pasaoglu, H. Barzegar, O.O. Teber, R. Kaya, M. Bastug, A. Khataee, I. Koyuncu, Cellulose acetate in fabrication of polymeric membranes: a review, Chemosphere, 295 (2022) 133914, doi: 10.1016/j.chemosphere.2022.133914.
[11] C. Lavanya, R. Geetha Balakrishna, K. Soontarapa, M.S. Padaki, Fouling resistant functional blend membrane for removal of organic matter and heavy metal ions, J. Environ. Manage., 232 (2019) 372–381.
[12] J. Zhu, J. Hou, Y. Zhang, M. Tian, T. He, J. Liu, V. Chen, Polymeric antimicrobial membranes enabled by nanomaterials for water treatment, J. Membr. Sci., 550 (2018) 173–197.
[13] Y. Ibrahim, E. Abdulkarem, V. Naddeo, F. Banat, S.W. Hasan, Synthesis of super hydrophilic cellulose-alpha zirconium phosphate ion exchange membrane via surface coating for the removal of heavy metals from wastewater, Sci. Total Environ., 690 (2019) 167–180.
[14] R.T. Thomas, J.I. Del Río de Vicente, K. Zhang, M. Karzarjeddi, H. Liimatainen, K. Oksman, Size exclusion and affinity-based removal of nanoparticles with electrospun cellulose acetate membranes infused with functionalized cellulose nanocrystals, Mater. Des., 217 (2022) 110654, doi: 10.1016/j.matdes.2022.110654.
[15] P. Kanagaraj, I.M.A. Mohamed, W. Huang, C. Liu, Membrane fouling mitigation for enhanced water flux and high separation of humic acid and copper ion using hydrophilic polyurethane modified cellulose acetate ultrafiltration membranes, React. Funct. Polym., 150 (2020) 104538, doi: 10.1016/j.reactfunctpolym.2020.104538.
[16] X. Lin, Y. He, Y. Zhang, W. Yu, T. Lian, Sulfonated covalent organic frameworks (COFs) incorporated cellulose triacetate/cellulose acetate (CTA/CA)-based mixed matrix membranes for forward osmosis, J. Membr. Sci., 638 (2021) 119725, doi: 10.1016/j.memsci.2021.119725.
[17] M.C. Andrade, J.C. Pereira, N. de Almeida, P. Marques, M. Faria, M. Clara Gonçalves, Improving hydraulic permeability, mechanical properties, and chemical functionality of cellulose acetate-based membranes by co-polymerization with tetraethyl orthosilicate and 3-(aminopropyl)triethoxysilane, Carbohydr. Polym., 261 (2021) 117813, doi: 10.1016/j.carbpol.2021.117813.
[18] H. Guo, Y. Peng, Y. Liu, Z. Wang, J. Hu, J. Liu, Q. Ding, J. Gu, Development and investigation of novel antifouling cellulose acetate ultrafiltration membrane based on dopamine modification, Int. J. Biol. Macromol., 160 (2020) 652–659.
[19] K.A. Gebru, C. Das, Humic acid removal using cellulose acetate membranes grafted with poly(methyl methacrylate) and aminated using tetraethylenepentamine, J. Environ. Manage., 217 (2018) 600–610.
[20] K. Rambabu, S. Gokul, A.S. Russel, A. Sivaramakrishna, B. Ponnusami, F. Banat, Lithium perchlorate modified nanoporous polyethersulfone membranes for improved dye rejection, Desal. Water Treat., 122 (2018) 146–157.
[21] S. Velu, K. Rambabu, P. Monash, C. Sharma, Improved hydrophilic property of PES/PEG/$MnCO_3$ blended membranes for synthetic dye separation, Int. J. Environ. Stud., 75 (2018) 592–604.
[22] K. Rambabu, S. Velu, A.V.P. Gurumoorthy, Cellulose acetate/poly(ethylene glycol)/iron oxide composite membranes for improved dye removal, Res. J. Pharm. Biol. Chem. Sci., 7 (2016) 552–560.
[23] J. Yuan, D. Mecerreyes, M. Antonietti, Poly(ionic liquid)s: an update, Prog. Polym. Sci., 38 (2013) 1009–1036.
[24] L. Yu, Y. Zhang, Y. Wang, H. Zhang, J. Liu, High flux, positively charged loose nanofiltration membrane by blending with poly(ionic liquid) brushes grafted silica spheres, J. Hazard. Mater., 287 (2015) 373–383.
[25] Y.-Y. Cheng, C.-H, Du, C.-J. Wu, K.-X. Sun, N.-P. Chi, Improving the hydrophilic and antifouling properties of poly(vinyl chloride) membranes by atom transfer radical polymerization grafting of poly(ionic liquid) brushes, Polym. Adv. Technol., 29 (2018) 623–631.
[26] S. Chen, J. Zheng, L. Li, S. Jiang, Strong resistance of phosphorylcholine self-assembled monolayers to protein adsorption: insights into nonfouling properties of zwitterionic materials, J. Am. Chem. Soc., 127 (2005) 14473–14478.
[27] Y.-L. Zhu, Z.-Y. Lu, Z.-W. Li, Z.-Y. Sun, X. Liu, Effect of the self-assembled structures of hydrated polyzwitterionic and polyanionic brushes on their self-cleaning capabilities, Langmuir, 35 (2019) 6669–6675.
[28] A. Zhu, Z. Wang, P. Li, X. Zhou, S. Shen. Preparation of a positive porous polyvinylidene fluoride membrane and its removal of mercury containing wastewater, Desal. Water Treat., 287 (2023) 59–66.
[29] S. Shen, L. Zhang, Y. Zhang, G. Zhang, J. Yang, R. Bai, Fabrication of antifouling membranes by blending poly(vinylidene fluoride) with cationic polyionic liquid, J. Appl. Polym. Sci., 137 (2020) 48878, doi: 10.1002/app.48878.
[30] L. Zhang, S. Shen, Y. Zhang, X. Zhou, R. Bai, Modification of polyvinylidene fluoride membrane by blending with cationic polyionic liquid, Desal. Water Treat., 189 (2020) 119–125.
[31] Z. Wang, S. Shen, L. Zhang, A. Ben Hida, G. Zhang, Hydrophilic and positively charged polyvinylidene fluoride membranes for water treatment with excellent anti-oil and anti-biocontamination properties, Membranes, 12 (2022) 438, doi: 10.3390/membranes12040438.
[32] A. Avornyo, A. Thanigaivelan, R. Krishnamoorthy, S.W. Hassan, F. Banat, Ag-CuO-decorated ceramic membranes for effective treatment of oily wastewater, Membranes, 13 (2023) 176, doi: 10.3390/membranes13020176.
[33] K. Rambabu, G. Bharath, P. Monash, S. Velu, F. Banat, Mu. Naushad, G. Arthanareeswaran, P.L. Show, Effective treatment of dye polluted wastewater using nanoporous $CaCl_2$ modified polyethersulfone membrane, Process Saf. Environ. Prot., 124 (2019) 266–278.
[34] K. Rambabu, S. Velu, Improved performance of $CaCl_2$ incorporated polyethersulfone ultrafiltration membranes, Period. Polytech., Chem. Eng., 60 (2016), doi: 10.3311/PPch.8482.
[35] M.D. Ong, I. Vasquez, B. Alvarez, D.R. Cho, M.B. Williams, D. Vincent Jr., Md. Arafat Ali, N. Aich, A.H. Pinto, M.R. Choudhury, Modification of cellulose acetate microfiltration membranes using graphene oxide–polyethyleneimine for enhanced dye rejection, Membranes, 13 (2023) 143, doi: 10.3390/membranes13020143.
[36] G. Mahmodi, R.R. Bafti, N.I. Boroujeni, S. Pradhan, S. Dangwal, B. Sengupta, V. Vatanpour, M. Sorci, M. Fathizadeh, P. Bikkina, G. Belfort, M. Yu, S.-J. Kim, Improving cellulose acetate mixed matrix membranes by incorporating hydrophilic MIL-101(Cr)-NH_2 nanoparticles for treating dye/salt solution, Chem. Eng. J., 477 (2023) 146736, doi: 10.1016/j.cej.2023.146736.